We are IntechOpen, the world's leading publisher of Open Access books Built by scientists, for scientists

4,800
Open access books available

122,000
International authors and editors

135M
Downloads

Our authors are among the

154
Countries delivered to

TOP 1%
most cited scientists

12.2%
Contributors from top 500 universities

CLARIVATE ANALYTICS BOOK CITATION INDEX INDEXED

WEB OF SCIENCE™

Selection of our books indexed in the Book Citation Index in Web of Science™ Core Collection (BKCI)

Interested in publishing with us?
Contact book.department@intechopen.com

Numbers displayed above are based on latest data collected.
For more information visit www.intechopen.com

Image Processing Techniques for Unsupervised Pattern Classification

C. Botte-Lecocq, K. Hammouche, A. Moussa, J.-G. Postaire, A. Sbihi & A. Touzani
University of Science and Technology of Lille
France

1. Introduction

The aim of cluster analysis is to divide a set of multidimensional observations into subsets according to their similarities and dissimilarities. These observations are generally represented as data points scattered through an N-dimensional data space, each point corresponding to a vector of observed features measured on the objects to be classified. In the framework of the statistical approach, many clustering procedures have been proposed, based on the analysis of the underlying probability density function (pdf) (Devijver & Kittler, 1982).

Independently from cluster analysis, a large amount of research effort has been devoted to image segmentation. To humans, an image is not just an unstructured collection of pixels. We generally agree about the different regions constituting an image due to our visual grouping capabilities. Among the factors that lead to such perceptual grouping, the most important are similarity, proximity and connectedness. The segmentation process can be considered as a partitioning scheme such that:

-Every pixel of the image must belong to a region,
-The regions must be composed of contiguous pixels,
-The pixels constituting a region must share a given property of similarity.

These three conditions can be easily adapted to the clustering process. Indeed, each data point must be assigned to a cluster, and the clusters must be composed of neighbouring data points since the points assigned to the same cluster must share some properties of similarity. Considering this analogy between segmentation and clustering, some image segmentation procedures based on the gray-level function analysis can be adapted to multidimensional density function analysis for pattern classification, assuming there is a one-to-one correspondence between the modes of the underlying pdf and the clusters.

In this framework of unsupervised pattern classification, the underlying pdf is estimated on a regular discrete array of sampling points (Cf. section 2). The idea of using a pdf estimation for mode seeking is not new (Parzen, 1962) and, in very simple situations, the modes can be detected by thresholding the pdf at an appropriate level, using a procedure similar to image binarization. A solution for improving this thresholding scheme is to adapt a probalistic labelling scheme directly derived from image processing techniques (Cf. section 3).

Source: Scene Reconstruction, Pose Estimation and Tracking, Book edited by: Rustam Stolkin,
ISBN 978-3-902613-06-6, pp.530, I-Tech, Vienna, Austria, June 2007

In the clustering context, a mode boundary is similar to a region boundary in an image since it is an area where abrupt local changes occur in the pdf. The modes of a distribution of multidimensional observations can then be detected by means of generalized gradient operators (Cf. section 4). Although these spatial operators enhance substantially the discontinuities that delineate the modes, a relaxation labeling process, similar to the one used for thresholding, can be necessary for mode boundary extraction.
Beside procedures based on the concepts of similarity and discontinuity, mathematical morphology has proven to be a valuable approach for image segmentation. This theory is adapted to cluster analysis by considering the sets of multidimensional observations as mathematical discrete binary sets (Cf. section 5).
Another approach is to consider statistical texture measures to describe the spatial distribution of the data points. Similarly to texture segmentation, the approach consists first of selecting a set of features that characterize the local distribution of the data points in the multidimensional data space in terms of textures. The data points with similar local textures are aggregated to define compact connected components of homogeneous textures considered as the cores of the clusters (Cf. section 6).
Modeling spatial relationships between pixels by means of Markov random fields has proved to be relevant to the image segmentation problem. The Markovian approach can also be adapted to the mode detection problem in cluster analysis (Cf. section 7).
The algorithms presented in this chapter must be tuned carefully in order to detect the significant modes of the distributions (Cf. section 8). The observations falling in these detected cluster cores are considered as prototypes so that the remaining data points are finally assigned to their respective clusters by means of classical supervised procedures (Cf. section 9).

2. Discretization of the data set

In order to adapt image processing tools to clustering, it is necessary to introduce a discrete array of sampling points. Let us consider Q observations $Y_q = [y_{q,1}, y_{q,2}, \ldots, y_{q,n}, \ldots, y_{q,N}]^T$, q=1 ,2 ,…, Q, where $y_{q,1}, y_{q,2}, \ldots, y_{q,n}, \ldots, y_{q,N}$ are the N coordinates of the observation Y_q in the data space. The range of variation of each component of the observations is normalized to the interval [0, K], where K is an integer, by means of the transformation:

$$y'_{q,n} = K \frac{y_{q,n} - \min_{q=1}^{q=Q}\{y_{q,n}\}}{\max_{q=1}^{q=Q}\{y_{q,n}\} - \min_{q=1}^{q=Q}\{y_{q,n}\}}.$$

Let $Y'_q = [y'_{q,1}, y'_{q,2}, \ldots, y'_{q,n}, \ldots, y'_{q,N}]^T$, q=1,2, ..., Q , be the Q new observations in the normalized data space. Each axis of this space is partitioned into K exclusive and adjacent intervals of unit width. This discretization defines an array of K^N hypercubes of unit side length. The centers of these hypercubes constitute a regular lattice of sampling points denoted P_r, $r=1,2,\ldots,K^N$. The unit hypercubic cell centered at point P_r is denoted $H(P_r)$. It is defined by its coordinates $h_{r,1}, h_{r,2}, \ldots, h_{r,n}, \ldots, h_{r,N}$, which are the integer parts of the

coordinates of its center P_r. The q^{th} normalized observation Y'_q falls into the unit cell $H(P_r)$ of coordinates $h_{r,n} = \text{int}(y'_{q,n})$, $n=1,2,...,N$, where $\text{int}(y'_{q,n})$ denotes the integer part of the real number $y'_{q,n}$.

Taking the integer parts of the coordinates of all the available normalized observations yields the list of the non-empty cells whose coordinates are defined on the set Z^{+N}. If several observations fall into the same cell, this one appears many times in the list of non-empty cells. It is easy to determine the number $q[H(P_r)]$ of observations that fall into the hypercubic cell of center P_r by counting the number of times the cell $H(P_r)$ appears in that list (Postaire & Vasseur, 1982). Subsequently, the distribution of the data points can be approximated by the discrete multi-dimensional histogram $\hat{p}(P_r) = q[H(P_r)]$. Note that $\hat{p}(P_r)/Q$ can be considered as an approximate value of the underlying pdf at point P_r.

The result of this sampling procedure is a multidimensional regular array of discrete integers in the range [0, p_{max}], where p_{max} is the maximum value of $\hat{p}(P_r)$, $r = 1,2,...,K^N$, that is well conditioned for a multidimensional analysis. Let $\underline{X}$ denote the set of the centers X of the non-empty hypercubic cells defined by this procedure.

3. Mode detection by relaxation

In very simple situations, the modes can be detected by thresholding the pdf at an appropriate level, using a procedure similar to image binarization. A «mode» label is associated with each point where the underlying pdf is above the threshold. Otherwise, the corresponding point is assigned a «valley» label.

However, in practical situations, it is often difficult, or even impossible, to select an appropriate threshold to detect the significant modes. A solution for improving this simple thresholding scheme is to consider the spatial relationships among the sampling points where the underlying pdf is estimated, rather than making a decision at each point independently of the decisions at other points. Probabilistic labelling, or relaxation, is a formalism through which object labels are iteratively updated according to a compatibility measure defined among the neighbouring labels (Hummel & Zucker, 1983). This approach, which has been mainly applied to image processing (Rosenfeld & Smith, 1981), has been adapted to cluster analysis to reduce local ambiguities in the mode/valley discrimination process (Touzani & Postaire, 1988).

To convey the general idea of the relaxation labelling procedure, which has been applied to a variety of image processing problems, we initially assign to each sampling point P_r a probability $p_r^{(0)}(M)$ that it belongs to a mode. The initial probability that P_r belongs to a valley is therefore $p_r^{(0)}(V)=1-p_r^{(0)}(M)$. These probabilities are then adjusted in parallel on the basis of the probability assignments at the neighbouring points of P_r. The process is iterated and finally each sampling point P_r is assigned the "mode" or the "valley" label according to the resulting probabilities $p_r(M)$ and $p_r(V)$. To be more specific, the initial probability $p_r^{(0)}(M)$ that P_r belongs to a mode is given by:

$$p_r^{(0)}(M)=\frac{\hat{p}(P_r)-p_{min}}{p_{max}-p_{min}},$$

where p_{min} is the minimum value of the estimated pdf over the whole data space, generally equal to 0.

For each pair of neighbouring sampling points $\{P_r\ P_{r'}\}$, we define a measure $C_{rr'}(\lambda,\lambda')$ of compatibility between label λ assigned to point P_r and label λ' assigned to point $P_{r'}$, where λ and λ' can be either the "mode" or the "valley" labels, such as :

$$C_{rr'}(\lambda,\lambda')=\frac{\left[p_r(\lambda)-\overline{p}(\lambda)\right].\left[p_{r'}(\lambda')-\overline{p}(\lambda')\right]}{\left[p_{max}(\lambda)-\overline{p}(\lambda)\right].\left[p_{max}(\lambda')-\overline{p}(\lambda')\right]}$$

and where :

$p_r(\lambda)$ is the probability associated with label λ at point P_r

$$\overline{p}(\lambda)=(1/K^N)\sum_{r=1}^{K^N}p_r(\lambda)$$

$$p_{max}(\lambda)=\max_r\{p_r(\lambda)\},\ r=1,2,...,K^N.$$

At the $(t+1)^{th}$ iteration, the new estimate of the probability of label λ at point P_r is updated as :

$$p_r^{(t+1)}(\lambda)=\frac{p_r^{(t)}(\lambda)\left[1+q_r^{(t)}(\lambda)\right]}{p_r^{(t)}(M)\left[1+q_r^{(t)}(M)\right]+p_r^{(t)}(V)\left[1+q_r^{(t)}(V)\right]}$$

where :

$$q_r^{(t)}(\lambda)=\frac{1}{(2\delta+1)^N}\sum_{\substack{P_{r'}\in V_\delta(P_r)\\ r'\neq r}}\left\{\rho(\lambda,M)C_{rr'}(\lambda,M)p_r^{(t)}(M)+\rho(\lambda,V)C_{rr'}(\lambda,V)p_r^{(t)}(V)\right\}.$$

$V_\delta(P_r)$ denotes the hypercubic neighbourhood of point P_r, of size $2\delta+1$ where δ is an integer, consisting of $(2\delta+1)^N$ neighbouring points, defined as :

$$V_\delta(P_r)=\left\{[x_1,...,x_N]^T\ /\ h_{r,i}-\delta<x_i<h_{r,i}+\delta;i=1,2,....,N\right\}$$

The weighting coefficients $\rho(\lambda,M)$ and $\rho(\lambda,V)$ must satisfy the condition:

$$\sum_{\lambda\in\{M,V\}}\left[\rho(\lambda,M)+\rho(\lambda,V)\right]=1.$$

When convergence of the sequence of probabilities $p_r^{(t)}(M)$ is completed, a value of 1 indicates an unambiguous "mode" label while a value of 0 indicates an unambiguous "valley" label. Experiments show that most label probabilities reach these extreme values after a few iterations. However, in some cases, the limiting values may be strictly between 0 and 1 but, due to the drastic reduction of ambiguities, thresholding these probabilities becomes trivial.

Figure 1 (b) shows a raw estimate of the pdf corresponding to 1000 bidimensional observations of figure 1 (a) distributed as three clusters of unequal weights. The probabilities at the last step of the relaxation process are displayed in figure 1 (c). This example demonstrates the considerable noise cleaning of the relaxation process.

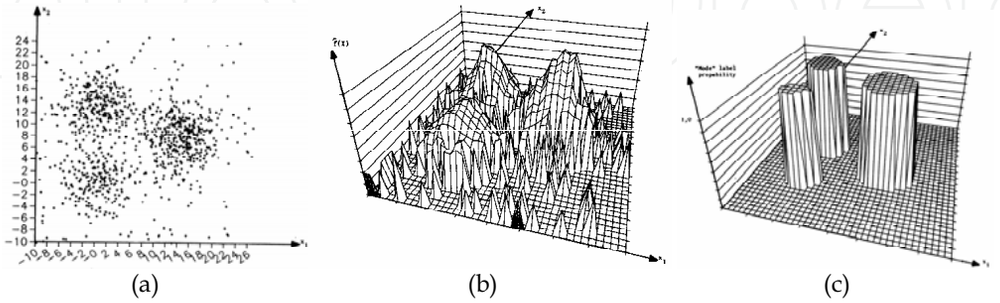

(a) (b) (c)

Figure 1. Mode detection by relaxation

(a) Scatter diagram of the data set
(b) Raw estimate of a bidimensional pdf
(c) Label probability diagram at the last iteration of the relaxation process

4. Mode boundary detection

4.1 Multidimensional differential operators

The segmentation of an image can be considered as a problem of edge detection. Similarly, in the clustering context, a mode boundary can be defined as an area of abrupt local changes in the pdf. It can be detected by means of generalized gradient operators designed to perform a discrete spatial differentiation of the estimated pdf (Touzani & Postaire, 1989).
In an N-dimensional space, the Robert's operator (Davis, 1975) is generalized by computing the $N(N-1)/2$ elementary gradients defined by :

$$\hat{G}_{\alpha,\beta}(P_r)=\left|\hat{p}(h_{r,1},....,h_{r,\alpha},....,h_{r,\beta},....,h_{r,N})-\hat{p}(h_{r,1},....,h_{r,\alpha}+1,....,h_{r,\beta}+1,....,h_{r,N)}\right|$$
$$+\left|\hat{p}(h_{r,1},....,h_{r,\alpha}+1,....,h_{r,\beta},....,h_{r,N})-\hat{p}(h_{r,1},....,h_{r,\alpha},....,h_{r,\beta}+1,....,h_{r,N})\right|$$

where $\alpha=1,2,....,N$, $\beta=1,2,....,N$, $\alpha\neq\beta$.

Thanks to the algorithm used for pdf estimation, which yields the list of the nonempty hypercubes, the gradient operator is only applied to non empty regions of the data space, thus speeding up the procedure.
Another way to estimate the gradient of a multidimensional pdf is to generalize the Prewitt's operator by determining the hyperplane that best fits the estimated function $\hat{p}(P_r)$ at point P_r (Morgenthaler & Rosenfeld, 1981). This hyperplane, defined by:

$$\Pi(x_1,....,x_N)\equiv a_0+\sum_{i=1}^{N} a_i\, x_i$$

is found by minimizing the squared error :

$$E_{rr} = \int_{V_\delta(P_r)} (\Pi(x_1,....,x_N) - \hat{p}(x_1,....,x_N)^2 \, dx_1....dx_N$$

Setting the origin at point P_r and then differentiating E_{rr} with respect to $a_0,....,a_N$ and setting the result to zero yields the coefficients of the hyperplane. In the discrete case, we obtain:

$$a_n = \frac{\sum_{P_r \in V_\delta(P_r)} h_{r',n} \hat{p}(h_{r',1},....,h_{r',N})}{\sum_{P_r \in V_\delta(P_r)} (h_{r',n})^2} \quad , n = 0,1,2,....,N \; .$$

Analogously to Robert's operator, Prewitt's operator is just applied in non empty regions of the data space.

The sampling points that have high gradient values are possible boundary elements. Since mode boundaries are closed hypersurfaces, the boundary extraction procedure must be an omnidirectional aggregation process. The candidate points lying in the neighbourhood of a current boundary point are evaluated on the basis of their satisfying a gradient magnitude criterion for acceptance. To be more specific, let $\hat{G}(P_0)$ be the estimated magnitude of the gradient at the starting point P_0 and let τ be a tolerance factor, so that the aggregation algorithm incorporates only points with gradient magnitude greater than the threshold value $\tau.\hat{G}(P_0)$. When the algorithm is successful in finding some boundary elements in the neighbourhood of the current point, these elements are added to the currently accepted piece of boundary and become available current points for the next stages of the growth process. If there are no acceptable candidates in the neighbourhoods of all available current points, the aggregation terminates. The aggregation algorithm is then reinitialised from a new starting point, which is the point with the highest gradient value among the points that do not belong to a reconstructed boundary.

The boundaries of the three clusters constituting the distribution of bidimensional observations of figure 2 (a) are displayed in figure 2 (b). They reflect the modal structure of the distribution and can be easily used to assign the data points to their respective clusters.

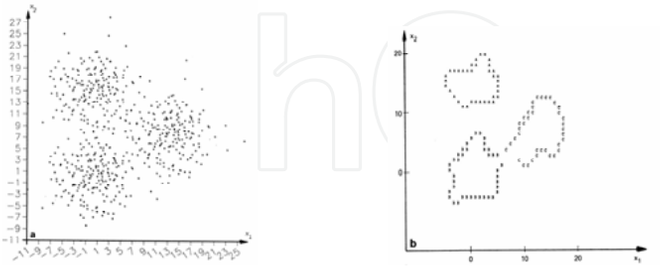

(a) (b)

Figure 2. Mode boundary detection

(a) Scatter diagram of a two-dimensional data set
(b) Detected mode boundaries

These mode boundaries can be used for unsupervised identification of normal mixtures (Postaire & Touzani, 1990).

4.2. Relaxation for boundary detection

Although these spatial operators enhance substantially the discontinuities that delineate the modes, a relaxation labeling process, similar to the one used for thresholding, can be necessary for mode boundary extraction (Postaire & Touzani, 1989).

Figure 3 (b) shows the response of the generalized Prewitt's operator on the data set of figure 3 (a). The result of figure 3 (c) shows how an iterative relaxation scheme can be used to enhance the mode boundaries while weakening the effects of noise and irregularities in the distribution of the input data.

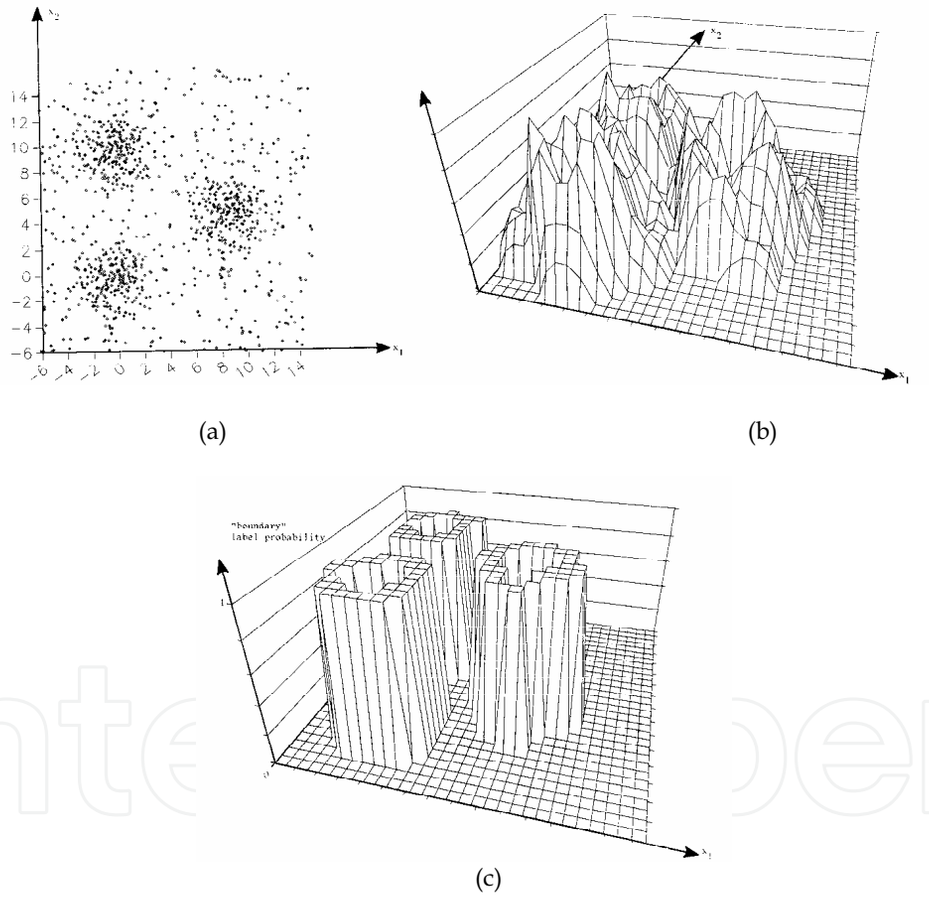

(a) (b)

(c)

Figure 3. Mode boundary detection by relaxation

(a) Scattered diagram of the data set
(b) Response of the generalized Prewitt's operator
(c) Result of 6 iterations of the relaxation process

5. Mode detection by morphology

5.1. Introduction

Mathematical morphology has been developed as an algebra of set-theoretic operations in Euclidean spaces for quantitative description of geometrical structures. As introduced by Matheron and Serra (Matheron, 1985) (Serra, 1987), this approach has been mainly concerned with binary and graylevel image analysis. Erosions, dilations, openings and closings are the simplest transformations derived from mathematical morphology but other transformations such as thinnings and thickenings are also widely used.

These operations can be adapted to cluster analysis by considering the set $\underline{X}$ of centers X of non empty hypercubes, determined from the data by means of the discretization procedure described in section 2, in terms of a mathematical set in a Z^{+N} space (Postaire et al., 1993). The underlying pdf is then viewed as a closed set in the Euclidean space $E = Z^{+N} \times R^{+*}$.

The structure of this discrete set $\underline{X}$ can then be analysed by means of binary morphological operations, in order to extract the significative connected components of $\underline{X}$, each connected component indicating the existence of a cluster in the original data set. Another approach consists of detecting the modes of the pdf by means of multivalued morphological transformations.

5.2. Binary morphology

The binary morphology is based on the comparison between the local structure of the discrete set $\underline{X}$, and the structure of a pre-specified subset $\underline{B}$, called structuring element, whose structure depends on the properties that have to be extracted from $\underline{X}$.

The dilation of $\underline{X}$ by a structuring element $\underline{B}$ is the Minkowski addition of $\underline{X}$ and $\underline{B}$, such as:

$$\underline{D} = \underline{X} \oplus \underline{B} = \bigcup_{B \in \underline{B}} \left(\underline{X}\right)_B = \left[D \in Z^N \middle| D = X + B, X \in \underline{X}, B \in \underline{B}\right].$$

The set $\underline{D}$ is found by translating $\underline{X}$ by all the elements of $\underline{B}$ and then taking the union. Dilation by a small compact structuring element can be used to expand the set $\underline{X}$. Dilation of $\underline{X}$ by $\underline{B}$ is the set $\underline{D}$ composed of all those elements D such as $\underline{B}$ translated to D intersects $\underline{X}$.

The erosion, which is the Minkowsky set subtraction of $\underline{B}$ from $\underline{X}$, is the operation dual to dilation with respect to complementation. It is defined by :

$$\underline{E} = \underline{X} \Theta \underline{B} = \bigcap_{B \in \underline{B}} \left(\underline{X}\right)_B = \left[E \in Z^N \middle| E + B = X, X \in \underline{X}, \text{for every } B \in \underline{B}\right]$$

The set $\underline{E}$ is found by translating $\underline{X}$ by all the elements of $\underline{B}$ and then taking the intersection. It consists of all the elements E for which $\underline{B}$ translated to E is contained in $\underline{X}$**.** Erosion by a compact structuring element $\underline{B}$ can be viewed as a shrinking transformation of the set $\underline{X}$.

In practice, erosion and dilation are seldom used alone. They are often combined in pairs, giving two other fundamental morphological operations called openings and closings.

The opening of $\underline{X}$ by $\underline{B}$, denoted $\underline{X}_{\underline{B}}$, is the set resulting from the erosion of $\underline{X}$ by $\underline{B}$, followed by the dilation of the eroded set by $\underline{B}$:

$$\underline{X}_{\underline{B}} = \underline{X} \Theta \underline{B} \oplus \underline{B}$$

At the completion of this sequence, the opening $\underline{X}_{\underline{B}}$ is generally different from $\underline{X}$. The opening suppresses irrelevant protuberant details of the set towards its boundary and yields a rather simplified version of $\underline{X}$.

By duality, the closing of $\underline{X}$ by $\underline{B}$, denoted $\underline{X}^{\underline{B}}$, is the result of first dilating $\underline{X}$ and then eroding the dilated set by $\underline{B}$:

$$\underline{X}^{\underline{B}} = \underline{X} \Theta \underline{B} \oplus \underline{B}$$

The closing tends to fill the holes and the gaps in the set $\underline{X}$.

The set $\underline{X}$ of figure 4 (a) is used to demonstrate the effects of these morphological transformations on bidimensional data. The opening and the closing of this discrete binary set by a (3x3) square structuring element are shown in figures 4 (b) and 4 (c), respectively.

The results show that these two transformations tend to produce new sets, with simpler shapes than the original ones. Opening and closing seem to be very effective to eliminate isolated groups of set points and holes, provided theses details do not exceed the size of the structuring element. All the irrelevant details are rubbed out, while the actual structure of the data remains unchanged.

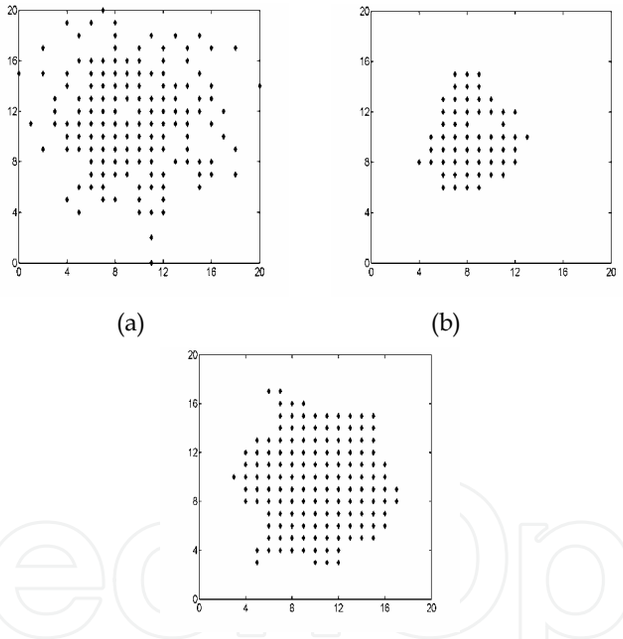

Figure 4. Morphological transformations of a binary set

(a) Binary discrete set (* are the centers of the non-empty hypercubes)
(b) Opened set using a compact 3x3 structuring element
(c) Closed set using a compact 3x3 structuring element

In order to extract the connected components of $\underline{X}$, the cluster detection procedure consists of successively applying opening and closing operations, removing irrelevant details in the discrete set structure while preserving the global shapes of unsuppressed components. The procedure has been applied to the raw data of figure 5 (a). The three cluster cores of figure 5 (b) have been obtained by a single opening operation followed by a closing operation.

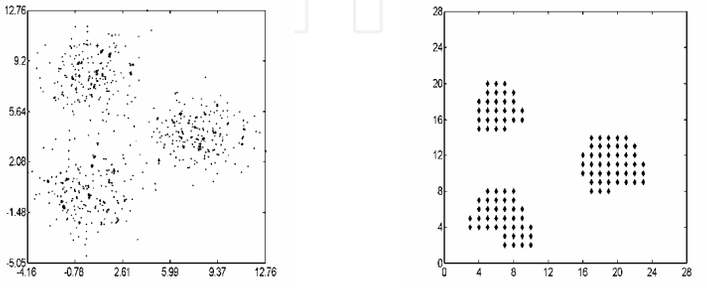

(a) (b)

Figure 5. Mode detection by binary morphology

(a) Raw bidimensional data set
(b) The three modes detected by an opening followed by a closing

The connected components of $\underline{X}$ can also be extracted by analysing the connectivity of $\underline{X}$ by means of a valley seeking technique using morphological thinnings (Botte-Lecocq & Postaire, 1994). Another solution is to extract the connected components of $\underline{X}$ by means of its ultimate eroded set (Benslimane et al. 1996).

5.3. Multivalue morphology

The binary morphological techniques, where only non-empty hypercubes are considered independently of the associated pdf value, are very simple to implement and very efficient unless the overlapping degree between the different clusters is small.

Modes can also be viewed as connected components in the space $E = Z^{+N} \times R^{+*}$ previously defined. If we consider the additive inverse of the pdf, each of its wells corresponds to a mode of the pdf, which can be detected by adapting watershed transforms (Meyer & Beucher, 1990), usually applied for two-dimensional image segmentation.

Let $f(X)$ be this additive inverse such as $f(X) = -\hat{p}(X)$. This function is shifted up so that its new version:

$$f^*(X) = -\hat{p}(X) + \left| \min_X \{-\hat{p}(X)\} \right| = -\hat{p}(X) + \max_X \{\hat{p}(X)\}$$

becomes positive with its absolute minimum at zero.

In image segmentation, the most commonly used algorithm for efficient divide determination consists of constructing a numerical skeleton by means of homotopic thinning transformations of the gray level function (Meyer, 1989). The idea behind this thinning process is to deepen the level of the function within the catchment basins so that

their bottoms become flat, while leaving unchanged the function along the divides separating these basins.

The thinning of a function consists in a morphological transformation using a composite structuring element $\underline{B}$ composed of two sets of configurations $\underline{B_0}$ and $\underline{B_1}$. $\underline{B_0}$ is the subset of points of $\underline{B}$ with a 0 value while $\underline{B_1}$ is the subset of the points with a 1 value in this composite structuring element. The application of the morphological transformation means that the structuring element $\underline{B}=(\underline{B_1},\underline{B_0})$ is moved systematically through the entire discretized data space so as to position it at every sampling point. The result of the thinning of the function $f^*(X)$ at the current position of the structuring element is given by:

$$\begin{cases} g(X)=\sup\limits_{X'\in\underline{B_0}}\left\{f^*(X')\right\} \text{ if and only if } \sup\limits_{X'\in\underline{B_0}}\left\{f^*(X')\right\}< f^*(X) \le \inf\limits_{X'\in\underline{B_1}}\left\{f^*(X')\right\} \\ g(X)=f^*(X) \text{ else.} \end{cases},$$

The interpretation of this morphological operation is clear. Let $\underline{B_X}=(\underline{B_1},\underline{B_0})_X=(\underline{B_1}_X,\underline{B_0}_X)$ be the structuring element whose origin is shifted to the current position $X\in\underline{X}$. By this translation of $\underline{B}$, if for any point X' falling in the part $\underline{B_1}_X$ of the composite structuring element $f^*(X)\ge f^*(X)$, and if for any point X'' falling in the other part $\underline{B_0}_X$ $f^*(X'') < f^*(X)$, then $f^*(X)$ is replaced by the supremum of the function inside the part $\underline{B_0}_X$ of the shifted structuring element. Otherwise, $f^*(X)$ is not modified.

Thinning transformations are generally used sequentially. A sequential thinning can be obtained as a sequence of eight elementary thinnings using the structuring elements $\underline{L^{(i)}}$, $i=1,2,...,8$ that are obtained by successive rotations by $\Pi/4$ of the composite structuring element $\underline{L^{(1)}}$ shown in figure 6 (a). A value of one indicates an element that belongs to part $\underline{L_1^{(1)}}$ of $\underline{L^{(1)}}$, while an element with a zero value belongs to part $\underline{L_0^{(1)}}$. The particular element denoted 1_0 is the center of the structuring element. An asterisk * in the matrix denotes an element belonging neither to $\underline{L_0^{(1)}}$ nor to $\underline{L_1^{(1)}}$.The transformations using this structuring family $L=\left\{\underline{L^{(1)}},...,\underline{L^{(8)}}\right\}$ preserve the connectivity properties of the data sets since they are homotopic. Hence, the sequential thinning is iterated and converges to the so-called homotopic skeleton. Idempotence is reached when two consecutive iterations yield the same result, and the thinning process is stopped.

This homotopic sequential thinning is performed with the *L* family (cf. figure 6 (a)). Each structuring element of this family is used to process the $N.(N-1)/2$ bi-dimensional discrete data sets lying in the planes containing the current point X where the operation is carried out and parallel to the planes defined by the axis of the data space taken two by two. That means that the thinning at any point X is obtained as a combination of $N.(N-1)/2$ elementary planar thinnings operating in orthogonal directions. This procedure circumvents the difficulty of finding composite structuring elements in N dimensions that would lead to homotopic transformations. As these elementary operations are commutative and

associative, they are combined in a single N-dimensional hypercubic composite structuring element of size 3. The orthogonal planes, containing the center of this hypercube and parallel to the planes defined by the axis taken two by two, have the structure of the considered plane structuring element of the *L* family. All the other elements constituting this N-dimensional hypercubic structuring element will be assigned an asterisk, as they are not used in the thinning process.

0	0	0
*	1_0	*
1	1	1

(a)

0	0	0
0	1_0	*
0	0	*

(b)

Figure 6. 2-D composite structuring elements from the Golay alphabet (Golay, 1969).

(a) The $\underline{L}^{(1)}$ structuring element

(b) The $\underline{E}^{(1)}$ structuring element

Figure 7 (b) shows the effect of this sequential thinning on the pdf of figure 7 (a) when it is iterated until idempotence.

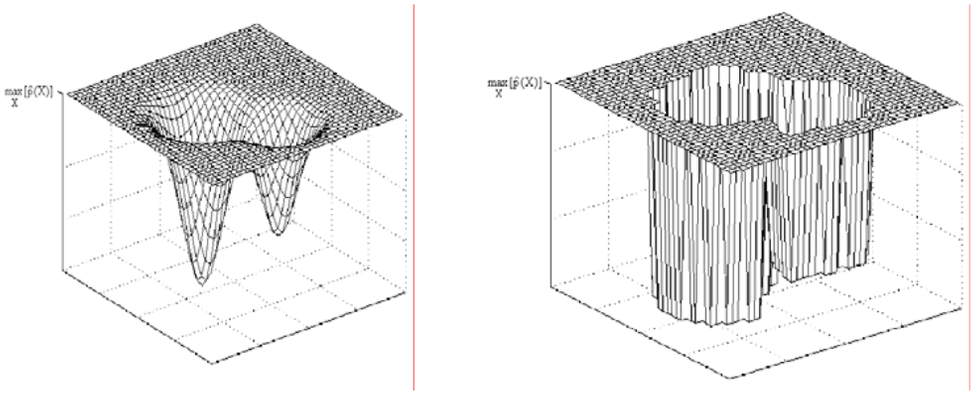

(a) (b)

Figure 7. Sequential thinning of the shifted additive inverse of a pdf with the *L* family

(a) Shifted additive inverse of a bimodal pdf

(b) Result of the last iteration of the thinning process corresponding to idempotence

Note that the multidimensional skeletons resulting from the sequential thinning operations may present non-significant ramifications. They are removed by a pruning operation, performed by means of a sequential thinning with another family of structuring elements, i.e. the *E* structuring family, which is not homotopic (cf. figure 6 (b)). When sequentially thinning the function with the composite structuring family $E=\left\{\underline{E}^{(i)}\ ,\ i=1,2,...,8\right\}$, spurious divides are shortened from their free ends. If this pruning operation is iterated until stabilization of the result, only the true divides remain that are the true boundaries between the modes of the distribution.

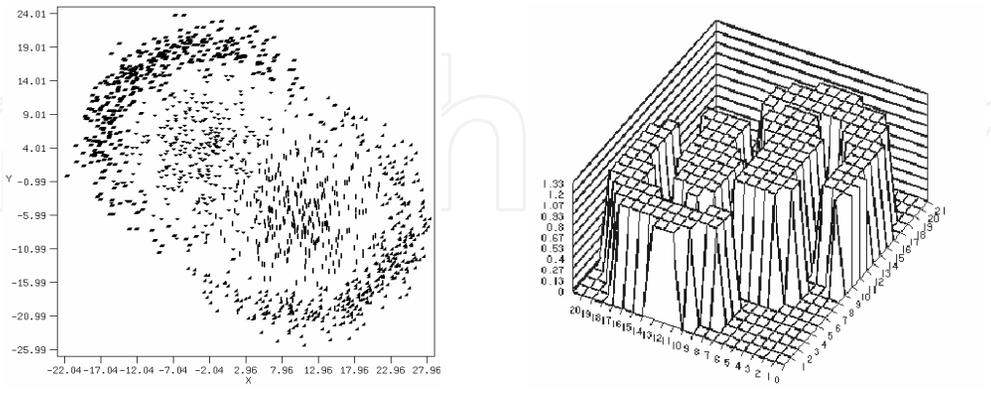

(a) (b)

Figure 8. Mode detection for a bidimensional data set
(a) Estimate of the multimodal underlying pdf
(b) Detected modal domains

The final thinned function consists of catchment basins separated by divides of unit width. Within a basin, the transformed function has a constant level equal to its local minimum value in the basin. The divides are easy to identify in the transformed function, since they are neighboured by catchment basins with lower levels. Figure 8 (b) shows the modes identified by means of this multidimensional watershed transform in the multidimensional pdf of figure 8 (a).

6. Clustering based on multidimensional texture analysis

Statistical texture measures can be used to describe the spatial distribution of the data points (Hammouche et al., 2006). Similarly to texture segmentation, the approach consists first of selecting a set of features that characterize the local distribution of the data points in the multidimensional data space in terms of textures. These textures, which reflect the spatial arrangement of data points, are then classified on the basis of these features. The data points with similar local textures are aggregated in the data space to define compact connected components of homogeneous textures. These multidimensional domains of uniform texture are finally considered as the modes of the distribution.

Textural properties are considered in terms of statistical models. The main difficulty is the selection of a set of relevant features to describe the properties of the spatial distribution of the observations. The concept of co-occurrence matrices, well-known in image processing, can be generalized to multidimensional data spaces. A large variety of features can then be derived from such matrices that combine spatial information with statistical properties (Haralick et al., 1973).

In the framework of image processing, an element $T(i,j)$ of a co-occurrence matrix is a count of the number of times a pixel $P_r = [x_{r,1}, x_{r,2}]^T$, with gray-level i, is positioned with respect to a pixel $P_{r'} = [x_{r',1}, x_{r',2}]^T$, with gray level j, such as :

$$P_{r'} = P_r + \begin{bmatrix} d\cos\theta \\ d\sin\theta \end{bmatrix}$$

where d is the distance in the direction θ between the two pixels.

A similar co-occurrence matrix can be determined to characterize the local distribution of the data points in a given neighbourhood of each non-empty hypercube. We use the classical hypercubic neighbourhood of side length $(2\delta+1)$ previously defined. As directionality and periodicity are obviously irrelevant characteristics of the data point distributions, it is not necessary to determine co-occurrence matrices for different sets of discrete values of the distance d and the orientation θ between the pairs of sampling points taken into account. Hence, only one co-occurrence matrix is determined for each sampling point. The co-occurrences $T(i,j)$ of any given pair (i, j) of discrete multidimensional histogram values such as $i=\hat{p}(P_r)$ and $j=\hat{p}(P_{r'})$, are simply counted for all the couples of adjacent sampling points encountered within this hypercubic neighbourhood. Two sampling points are considered as adjacent if they are the centers of two hypercubes that have at least one point in common. As the histogram $\hat{p}$ is quantized on a set of $p_{max}+1$ discrete values, the co-occurrence matrices have $p_{max}+1$ rows and $p_{max}+1$ columns.

Several local texture features can be computed from these specific co-occurrence matrices, which accumulate information on the data distribution in the neighborhood of each sampling point (Cf. Table 1). These features are expected to characterize such properties as roughness, smoothness, homogeneity, randomness or coarseness rather than textural properties such as directionality or periodicity, since each co-occurrence matrix summarizes the number of occurrences of pairs of histogram values for all possible pairs of adjacent sampling points lying within a given neighbourhood, without constraints on their orientations.

When the sampling points are characterized by a set of texture features, they can be represented as feature vectors in a multidimensional feature space. Texture classification consists of assigning the sampling points of the discrete data space to different texture classes defined in the feature space. This is an unsupervised classification problem since no a priori knowledge about the feature vectors associated with the textures to be identified is available. A simple solution is to use a well-established clustering procedure, such as the k-means algorithm.

Under the assumption that the cluster cores are multidimensional domains in the original data space, with homogeneous textures, it is expected that the hypercubes centered on sampling points assigned to the same class of texture give rise to connected components in the discrete data space. These components can be extracted by means of an aggregation procedure where two hypercubes whose centers belong to the same class of texture are assigned to the same component if they have at least one point in common. Small components resulting from this aggregation procedure may correspond to non-significant domains of the original data space containing only a small number of data points. Therefore, any domain containing less than 5% of the total number Q of observations is discarded.

Uniformity-1 (1st order)	$f_1 = \frac{1}{N_c}\sum_{i=0}^{P_{max}} T(i,i)$
Uniformity-2 (2nd order)	$f_2 = \frac{1}{N_c^2}\sum_{i=0}^{P_{max}} T(i,i)^2$
Homogeneity	$f_3 = \frac{1}{N_c}\sum_{i=0}^{P_{max}}\sum_{j=0}^{P_{max}} \frac{T(i,j)}{1+(i-j)^2}$
Correlation	$f_4 = \frac{1}{N_c}\sum_{i=0}^{P_{max}}\sum_{j=0}^{P_{max}} ijT(i,j)$
Energy	$f_5 = \frac{1}{N_c^2}\sum_{i=0}^{P_{max}}\sum_{j=0}^{P_{max}} T(i,j)^2$
Entropy	$f_6 = -\frac{1}{N_c}\sum_{i=0}^{P_{max}}\sum_{j=0}^{P_{max}} T(i,j)\log\left(T(i,j)/N_c\right)$
Inertia	$f_7 = \frac{1}{N_c}\sum_{i=0}^{P_{max}}\sum_{j=0}^{P_{max}} (i-j)^2 T(i,j)$
Means	$f_8 = \frac{1}{N_c}\sum_{i=0}^{P_{max}}\sum_{j=0}^{P_{max}} i*T(i,j)$ $\quad f_9 = \frac{1}{N_c}\sum_{i=0}^{P_{max}}\sum_{j=0}^{P_{max}} j*T(i,j)$
Covariance	$f_{10} = \frac{1}{N_c}\sum_{i=0}^{P_{max}}\sum_{j=0}^{P_{max}} (i-f_8)(j-f_9)T(i,j)$
Cluster shade	$f_{11} = \frac{1}{N_c}\sum_{i=0}^{P_{max}}\sum_{j=0}^{P_{max}} ((i-f_8)+(j-f_9))^3 T(i,j)$
Cluster prominence	$f_{12} = \frac{1}{N_c}\sum_{i=0}^{P_{max}}\sum_{j=0}^{P_{max}} ((i-f_8)+(j-f_9))^4 T(i,j)$
Absolute value	$f_{13} = \frac{1}{N_c}\sum_{i=0}^{P_{max}}\sum_{j=0}^{P_{max}} \lvert i-j \rvert\ T(i,j)$

Table 1. Statistical texture features ($N_c = \sum_{i=0}^{P_{max}}\sum_{j=0}^{P_{max}} T(i,j)$ is a normalizing parameter)

Among the remaining domains, those corresponding to the actual modes of the distribution are expected to be more compact than those corresponding to their boundaries or to the valleys between them. Hence, they can be discriminated from other connected components by analyzing their compactness defined as:

$$C = [\text{total number of hypercubes}] / [\text{number of boundary hypercubes}]^N$$

which is as much as high as the component is compact. In these conditions, mode detection is straightforward by simple thresholding of the compactness.
Figure 9 (b) shows the modes identified as domains of homogeneous texture detected in the data set of figure 9 (a).

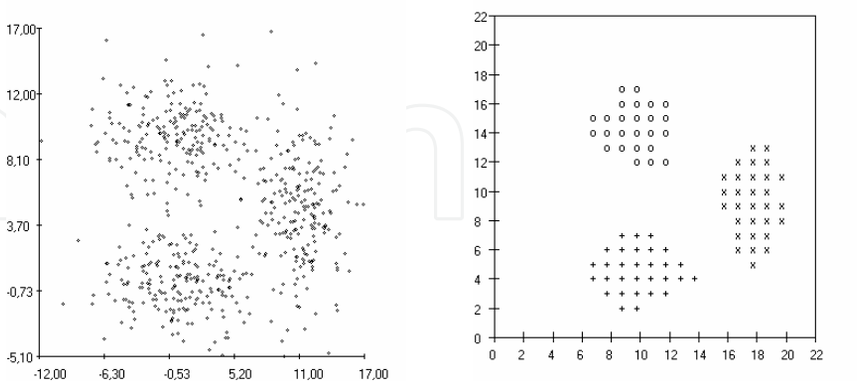

(a) (b)

Figure 9. Mode detection by texture analysis
(a) Data set
(b) Detected modes

7. Markov random field models for clustering

In the framework of the Markovian approach, each hypercube defined by the discretization process of section 2 corresponds to a site s whose coordinates are defined as the integer parts of the coordinates of its center. Let $\underline{S}$ denote the set of K^N sites defined in the data space. At each site s, $s=1,2,....,K^N$, a measure O_s is determined as :

$$O_s = \begin{cases} 1 & \text{if at least one observation falls into the site } s \\ 0 & \text{if the site } s \text{ is empty} \end{cases}$$

The resulting discrete binary set $O=\{O_s, s\in\underline{S}\}$ is the observable field which can be considered as a simplified binary representation of the distribution of the observations through the data space. This observable field O, which is composed of non-empty sites where $O_s = 1$ and empty sites where $O_s = 0$, is considered as an initial state of the hidden field Γ. In this initial hidden field, sites where $\Gamma_s = 1$ are considered as "mode sites"while, when $\Gamma_s = 0$, they are considered as "valley sites". As the field O is a simplified discrete binary version of the set of available observations, non-empty sites that belong to the modes tend to have a great number of non-empty sites among their nearest neighbours, due to the high concentration of observations within the modes. Similarly, empty sites tend to be more connected in the valleys than within the modes. In order to detect the modes of the distribution, the key problem is to assign the mode label to the sites that effectively define the modal domains and to assign the valley label to those that stand out of these modal domains (Sbihi et al., 2005).

A straightforward procedure for constructing connected subsets representing the modes in the data space is to use two sets of cliques (Moussa et al., 2001). For the sake of simplicity, let us consider an hypercubic neighbourhood $V_1(s)$ of side length 3 of each site s. The first set C_2^s is composed of the cliques c_2^s of size two that can be found in that neighbourhood and

that contain the site s itself (Cf. figure 10 (a)). $\varphi_{c_2^s}$ is the potential corresponding to these cliques. The second set $\overline{C}_2^s$ is composed of all the cliques $\overline{c}_2^s$ of size two that can be found in $V_1(s)$ and that do not contain the site s itself (Cf. figure 10 (b)). $\overline{\varphi}_{\overline{c}_2^s}$ is the potential function associated to these cliques. The resulting potential function is:

$$\varphi_{(c_2^s,\overline{c}_2^s)} = \upsilon\,\varphi_{c_2^s} + (1-\upsilon)\,\overline{\varphi}_{\overline{c}_2^s}$$

The factor $\upsilon = \dfrac{\alpha}{\alpha+\beta}$, where α is the number of cliques in $\overline{C}_2^s$ and β their number in C_2^s, weights the relative influence of the two terms, so that the measure of compatibility does not depend on the number of considered sites.

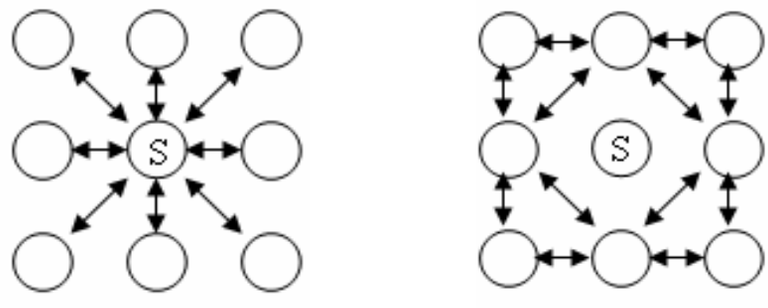

(a) (b)

Figure 10. The set of cliques in the bidimensional case

(a) The set C_2^s of cliques c_2^s related to the potential function $\varphi_{c_2^s}(.)$

(b) The set $\overline{C}_2^s$ of cliques $\overline{c}_2^s$ related to the potential function $\varphi_{\overline{c}_2^s}(.)$

All the sites are visited sequentially. The conditional energy $U(\Gamma_s = \gamma_s / \Gamma_r = \gamma_r, r \in V_1(s))$ is computed at each site s, taking into account the label configuration existing at that time for all its neighbouring sites. The label corresponding to the lowest conditional energy, which maximizes the Gibbs conditional probability:

$$P(\Gamma_s = \gamma_s / \Gamma_r = \gamma_r, r \neq s, r \in V_1(s)) = \frac{\exp[-U(\Gamma_s = \gamma_s / \Gamma_r = \gamma_r, r \in V_1(s))]}{\sum_{\gamma_n \in \{0,1\}} \exp[-U(\Gamma_s = \gamma_n / \Gamma_r = \gamma_r, r \in V_1(s))]}$$

is selected. The process is iterated until no further change occurs in the global energy, defined as:

$$U(\Gamma = \gamma) = \sum_{s \in S} \sum_{c_2^s \in C_2^s, \overline{c}_2^s \in \overline{C}_2^s} \varphi_{(c_2^s, \overline{c}_2^s)}$$

The algorithm stops when $\Delta^t = U^t - U^{t-1} = 0$, where U_t is the value of the global energy $U(\Gamma = \gamma)$ at iteration number t.

Figure 11 shows the modes that can be detected by modelling a bidimensional distribution as a Markovian process.

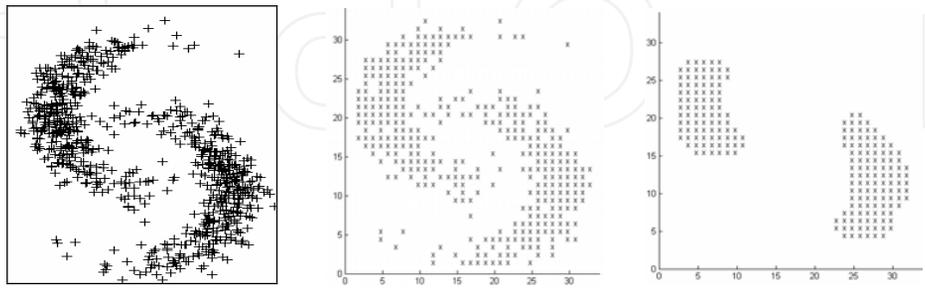

(a) (b) (c)

Figure 11. Mode detection by means of Markov Field Model

(a) Raw data set
(b) Sites where $O_s = 1$ in the observable field O
(c) Sites with the "mode" label in the hidden field Γ

8. Algorithms tunning

The performance of the above described algorithms depends mainly on the adjustment of the discretization parameter K and on the relevance of the chosen texture features.
Let us first consider the effect of the resolution of the discretization process. In fact, the adjustment of K depends on the sample size Q, on the dimensionality N of the data and on the structure of the distribution of the observations. It can be expected that, when true clusters exist, stable connected subsets of data points with similar properties appear for a wide range of values of K. Based on this assumption, the adjustment of K can be governed by the concept of cluster stability (Eigen et al., 1974). Choosing such a parameter in the middle of the largest range where the number of detected clusters remains constant, and different from one, has proved to be a good procedure to optimize a number of clustering algorithms when nothing is a priori known about the structure of the distribution of the observations (Postaire & Vasseur, 1981). Note that the larger the range is, the more reliable the tuning procedure is. Figure 12 shows the evolution of the number of detected modes with the discretization parameter K for the example of figure 9 (a). The largest range where this number remains constant appears for three modes. It is the reason why figure 9 (b) shows the detected modes in a discrete space with K=22, which is the middle of this range.
The concept of mode stability is very useful to improve the capabilities of clustering procedures. Indeed, in the specific framework of multidimensional texture analysis, the key problem is the selection of a set of suitable texture features. For choosing relevant features while reducing the dimensionality of the texture classification problem, a performance-dependent feature selection scheme, directly related to this concept, can be implemented. The effectiveness of a subset of features is evaluated by means of the width of the largest range of values of the discretization parameter K leading to the appropriate number of detected modes. As mentioned earlier, the larger this range, the more reliable the number of

detected modes. This criterion is used to select a set of relevant features among the available ones by means of a sequential forward selection technique (Siedlecki & Sklansky, 1988).

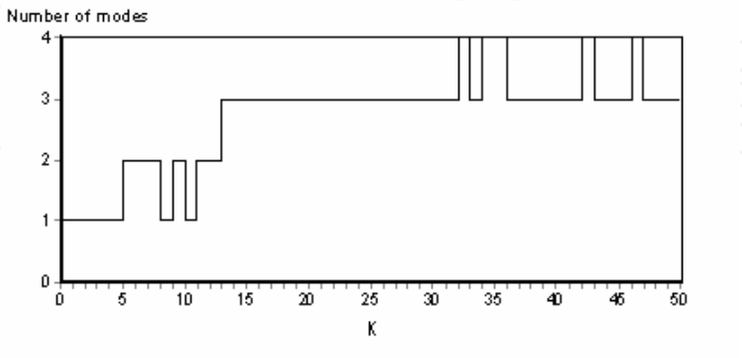

Figure 12. Effect of the parameter K on the number of detected modes

9. Final classification

Each detected mode reveals the presence of a cluster in the data space. Many grouping procedures can be used to assign the available observations to the so-detected clusters. One solution uses the input observations falling into the modal domains as prototypes. The remaining observations are finally assigned to the clusters attached to their nearest (Euclidean) neighbours among these prototypes (Cover & Hart, 1967).

When implementing this basic nearest neighbour classifier, experiments have shown that the results can be fairly improved if the remaining observations are assigned one by one to the clusters in a specific order depending on their distances to the prototypes (Gowda & Krishna, 1978). At each step of this procedure, we consider the distances between all the unassigned observations and all the prototypes. The smallest among these distances indicates the specific observation that must be considered. This observation is assigned to the cluster attached to its nearest neighbour and is integrated within the set of prototypes defining this cluster. This updating rule is iterated until all the observations are classified.

11. Conclusion and perspectives

All the clustering methods presented in this chapter tend to generalize bi-dimensional procedures initially developed for image processing purpose. Among them, thresholding, edge detection, probabilistic relaxation, mathematical morphology, texture analysis, and Markov field models appear to be valuable tools with a wide range of applications in the field of unsupervised pattern classification.

Following the same idea of adapting image processing techniques to cluster analysis, one of our other objectives is to model spatial relationships between pixels by means of other textural parameters derived from autoregressive models (Comer & Delp, 1999), Markov random fields models (Cross & Jain, 1983), Gabor filters (Jain & Farrokhnia, 1991), wavelet coefficients (Porter & Canagarajah, 1996) and fractal geometry (Keller & Crownover, 1989). We have also already started to work on the adaptation of fuzzy morphological operators to cluster analysis, by extracting the observations located in the modal regions performing an

adaptive morphological transformation of a fuzzy set, defined from the data set, with its associated mode membership function (Turpin et al., 1998). Face to these promising results, we are working on the introduction of fuzziness in other morphological operators such as fuzzy watersheds. Genetic algorithms, which have been used for image segmentation (Yin, 1999), are also powerfull tools that have to be tested.

12. References

Benslimane R., Botte Lecocq C. & Postaire J.-G. (1996) Extraction des modes en classification automatique par ligne de partage des eaux. *Journal Européen des Systèmes Automatisés*, Vol. 30, No 9, 1996, pp. 1169-1200

Botte-Lecocq C. & Postaire J.-G. (1991) Iterations of morphological transformations for cluster separation in pattern recognition, In: *Symbolic-Numeric Data Analysis and Learning,* pp. 173-185, Nova Science Pub., New York

Botte-Lecocq C. & Postaire J.-G. (1994) Mode detection and valley seeking by binary morphological analysis of connectivity for pattern classification, In: *New Approaches in Classification and Data Analysis*, pp. 194-203, Springer-Verlag, Berlin

Comer M. L. & Delp E. J. (1999) Segmentation of textured images using a multiresolution Gaussian autoregressive model. *IEEE Image Processing*, Vol. 8, 1999, pp. 408-420

Cover T. M. & Hart P. E. (1967) Nearest neighbor pattern classification. *IEEE Information Theory*, Vol. IT-13, No 1, 1967, pp. 21-27

Cross G. & Jain A. (1983) Markov random fields texture models. *IEEE Pattern Analysis and Machine Intelligence*, Vol. PAMI-5, 1983, pp. 25-39

Davis, L. S. (1975) A survey of edge detection techniques. *Computer Graphics and Image Processing*, Vol. 4, 1975, pp. 248-270

Eigen D. J., Fromm F. R. & Northouse R. A. (1974) Cluster analysis based on dimensional information with application to unsupervised pattern classification. *IEEE Pattern Analysis and Machine Intelligence,* Vol. PAMI-4, 1974, pp. 284-294

Golay A. (1969) Hexagonal pattern transform. *IEEE Trans. on Computers*, Vol. 18, No 8, 1969, pp. 733-740

Gowda K. C. & Krishna G. (1978) Agglomerative clustering using the concept of mutual nearest neighbourhood. *Pattern Recognition*, Vol. 10, 1978, pp. 105-112

Hammouche K., Diaf M. & Postaire J.-G. (2006) A clustering method based on multidimensional texture analysis. *Pattern Recognition,* Vol. 39, 2006, pp. 1265-1277

Haralick R. M., Shanmugam K., Dinstein I. (1973) Texture features for image classification, *IEEE Trans. on Systems, Man and Cybernetics*. Vol. SMC-3, No 6, 1973, pp. 610-621

Hummel R.A. & Zucker S.W. (1983). On the foundations of relaxation labeling process. *IEEE Pattern Analysis and Machine Intelligence,* Vol. PAMI-5, No 3, 1983, pp. 267-286

Jain A. K. & Farrokhnia F. (1991) Unsupervised texture segmentation using Gabor filters. *Pattern Recognition*, Vol.24, 1991, pp. 1167-1186

Keller J. M. and Crownover R. M. (1989) Texture description and segmentation through fractal geometry. *CVGIP: Graphical Models and Image Processing*, Vol. 45, 1989, pp. 150-166

Mallat S. G. (1989) Multifrequency channel decomposition of images and wavelets models, Theory for multiresolution signal decomposition: the wavelet representation, *IEEE Trans. Acoustics, Speech and Signal Processing*, Vol. 37, 1989, pp. 2091-2110.

Matheron G. (1985) *Random sets and integral geometry*, Wiley, New York

Meyer F. (1989) Skeletons and Perceptual Graphs. *Signal Processing*, Vol. 16, No 4, 1989, pp. 335-363

Meyer F. and Beucher S. (1990) Morphological segmentation. *J. Visual Communication and Image Representation*, Vol. 1, No 1, 1990, pp. 21-46

Morgenthaler D.G. & Rosenfeld A. (1981) Multidimensional edge detection by hypersurface fitting. *IEEE Pattern Analysis and Mach. Intell.,* Vol. PAMI-3, No 4, 1981, pp. 482-486

Moussa A., Sbihi A. & Postaire J.-G. (2001) Classification automatique par extraction des noyaux des classes utilisant une approche Markovienne. Journal Européen des Systèmes Automatisés, APII-JESA, Vol. 35, n° 9, 2001, pp. 1073-1087

Parzen E. (1962) On estimation of a probability density function and mode. *Ann. Math. Statist.* Vol. 33, 1962, pp. 1065-1076

Porter R. & Canagarajah N. (1996) A robust automatic clustering scheme for image segmentation using wavelets. *IEEE Image Processing*, Vol. 5,1996, pp. 662-665

Postaire J.-G. & Vasseur C. (1981) An approximate solution to normal mixture identification with application to unsupervised pattern classification. *IEEE Pattern Analysis and Machine Intelligence,* Vol. PAMI-3, No 2, 1981, pp. 163-179

Postaire J.-G. & Vasseur C. (1982). A fast algorithm for non parametric density estimation. *IEEE Pattern Analysis and Machine Intelligence,* Vol. PAMI-4, No 6, 1982, pp. 663-666

Postaire J.-G. & Touzani A. (1989) Mode boundary detection by relaxation for cluster analysis. *Pattern Recognition*, Vol. 22, No 5, 1989, pp. 477-490

Postaire J.-G. & Touzani A. (1990). A sample-based approximation of normal mixtures by mode boundary extraction for pattern classification. *Pattern Recognition Letters,* Vol. 11, No 3, 1990, pp. 153-166

Postaire J.-G., Zhang R. D. & Botte Lecocq C. (1993). Cluster analysis by binary morphology. *IEEE Pattern Analysis and Machine Intelligence,* Vol. PAMI-15, No 2, 1993, pp. 170-180

Rosenfeld A. & Smith R.C. (1981). Thresholding using relaxation. *IEEE Pattern Analysis and Machine Intelligence,* Vol. PAMI-3, No 5, 1981, pp. 598-606

Sbihi A. & Postaire J.-G. (1995) Mode extraction by Multivalue Morphology for Cluster Analysis, In: *From Data to Knowledge: Theoretical and Practical Aspects of Classification,* W. Gaul and D. Pfeifer (Ed.), pp. 212-221, Springer, Berlin

Sbihi A., Moussa A., Benmiloud B. & Postaire J.-G. (2000) A markovian approach to unsupervised multidimensional pattern classification, In: *Data Analysis, Classification and Related Method,* H.A.L. Kiers, J.-P. Rasson, P.J.F. Groenen and M. Scheder (Ed.) pp. 247-254, Springer, Berlin

Sbihi M., Moussa A., Postaire J.-G. & Sbihi A. (2005) Approche Markovienne pour la classification automatique non supervisée de données multidimensionnelles. *Journal Européen des Systèmes Automatisés,* Vol. 39, No 9-10, 2005, pp.1133-1154

Serra J. (1988) *Image analysis and mathematical morphology : theoretical advances*, Vol. 2, Academic Press, New York

Siedlecki W. & Sklansky J. (1988) On automatic feature selection. *Int. J. Pattern Recognition Artificial Intelligence*, Vol. 2, No 2, 1988, pp. 197-220

Touzani A. & Postaire J.-G. (1988). Mode detection by relaxation. *IEEE Pattern Analysis and Machine Intelligence*, Vol. PAMI-10, No 6, 1988, pp. 970-978

Touzani A. & Postaire J.-G. (1989). Clustering by mode boundary detection. *Pattern Recognition Letters,* Vol. 9, No 1, 1989, pp. 1-12

Turpin-Dhilly S. & Botte-Lecocq C. (1998) Application of fuzzy mathemetical morphology for pattern classification. *Advances in Data Science and Classification, Proceeding of the 6th Conf. of International Federation of Classification Society, Springer,* 1998, pp 125-130

Yin P.-Y. (1999) A fast scheme for optimal thresholding using genetic algorithms. *Signal Processing*, Vol. 72, 1999, pp. 85-95

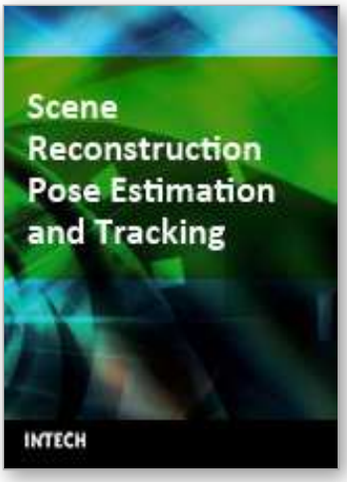

Scene Reconstruction Pose Estimation and Tracking

Edited by Rustam Stolkin

ISBN 978-3-902613-06-6

Hard cover, 530 pages

Publisher I-Tech Education and Publishing

Published online 01, June, 2007

Published in print edition June, 2007

This book reports recent advances in the use of pattern recognition techniques for computer and robot vision. The sciences of pattern recognition and computational vision have been inextricably intertwined since their early days, some four decades ago with the emergence of fast digital computing. All computer vision techniques could be regarded as a form of pattern recognition, in the broadest sense of the term. Conversely, if one looks through the contents of a typical international pattern recognition conference proceedings, it appears that the large majority (perhaps 70-80%) of all pattern recognition papers are concerned with the analysis of images. In particular, these sciences overlap in areas of low level vision such as segmentation, edge detection and other kinds of feature extraction and region identification, which are the focus of this book.

How to reference

In order to correctly reference this scholarly work, feel free to copy and paste the following:

C. Botte-Lecocq, K. Hammouche, A. Moussa, J.-G. Postaire, A. Sbihi and A. Touzani (2007). Image Processing Techniques for Unsupervised Pattern Classification, Scene Reconstruction Pose Estimation and Tracking, Rustam Stolkin (Ed.), ISBN: 978-3-902613-06-6, InTech, Available from: http://www.intechopen.com/books/scene_reconstruction_pose_estimation_and_tracking/image_processing_techniques_for_unsupervised_pattern_classification

INTECH
open science | open minds

InTech Europe
University Campus STeP Ri
Slavka Krautzeka 83/A
51000 Rijeka, Croatia
Phone: +385 (51) 770 447
Fax: +385 (51) 686 166
www.intechopen.com

InTech China
Unit 405, Office Block, Hotel Equatorial Shanghai
No.65, Yan An Road (West), Shanghai, 200040, China
中国上海市延安西路65号上海国际贵都大饭店办公楼405单元
Phone: +86-21-62489820
Fax: +86-21-62489821

IntechOpen